Figure 64 Fold A profile at grid reference 32422044, Khao Chan.

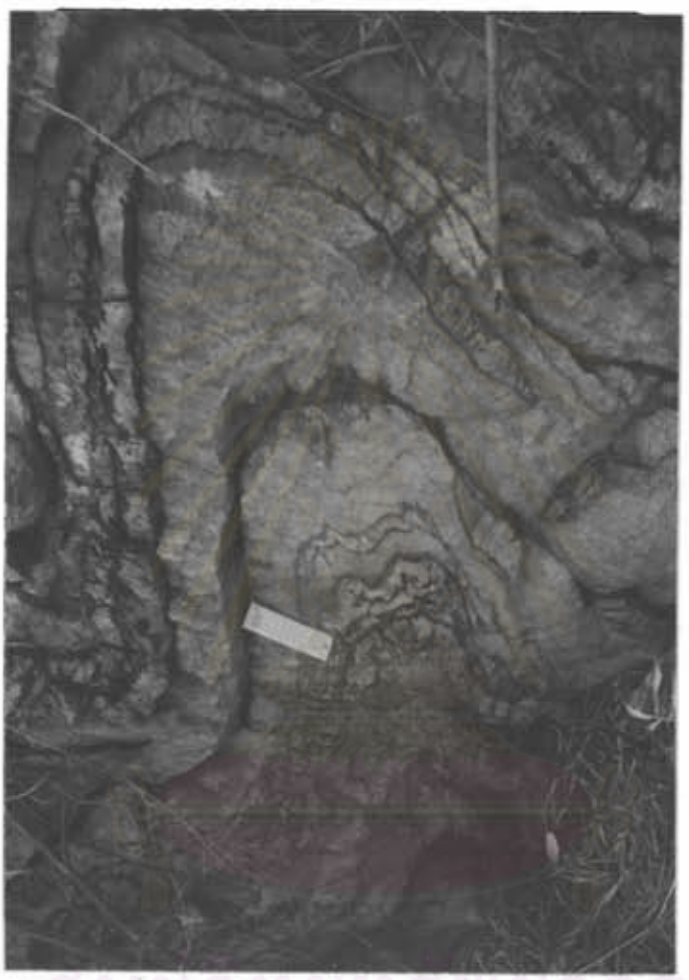

Figure 65 Fold B profile at grid reference 24031716, Khao Mai Nuan. (The scale is 15 cm long.)

normal and the tangential line to the folded horizon, measured at a point along the fold profile. Then the lines of equal dip, or dip isogons, joining the points of equal α on the upper-and lower-horizons (or bounding surfaces) of the same folded layer were drawn in the profiles (Figure 66). Furthermore, the thickness parallel to the axial trace, Tα, was measured at the various points in the profile, together with the orthogonal thickness, tα, measured as the shortest distance between the bounding surfaces. These give way to the parameters T'_α and t'_α where $T'_\alpha = T\alpha/To$ and $t'_\alpha = t\alpha/to$ (To and to are the corresponding values measured at the fold higne, thus To = to). All above fold elements (α, t'_α, T'_α and dip isogons) help classifying the folds according to their exact shape. The further explanation for the folding mechanism, etc., hence follows once the classes of the folds are identified. The fold elements measured in this study are collected in Table 4 while Figure 67 illustrates the fold classes from 2 localities in the study area.

The fold profiles show in Figure 66 indicate that the chert layers and limestones beds in Figure 65 were progressively developing to be an M-type. Therefore, two fold profiles, Folds B - 1 and B - 2 were drawn to study the dip isogon patterns. The aim of this method is to accurately analyzed and further interpreted these minor folds.

Based on the findings above, the patterns of isogons in both fold profiles are different (Figure 66). Fold A is mostly characterized by the weakly convergent and divergent isogons, while the isogons of the other two fold profiles, B - 1 and B - 2, were weakly convergent, similar-fold and weakly divergent isogons. The

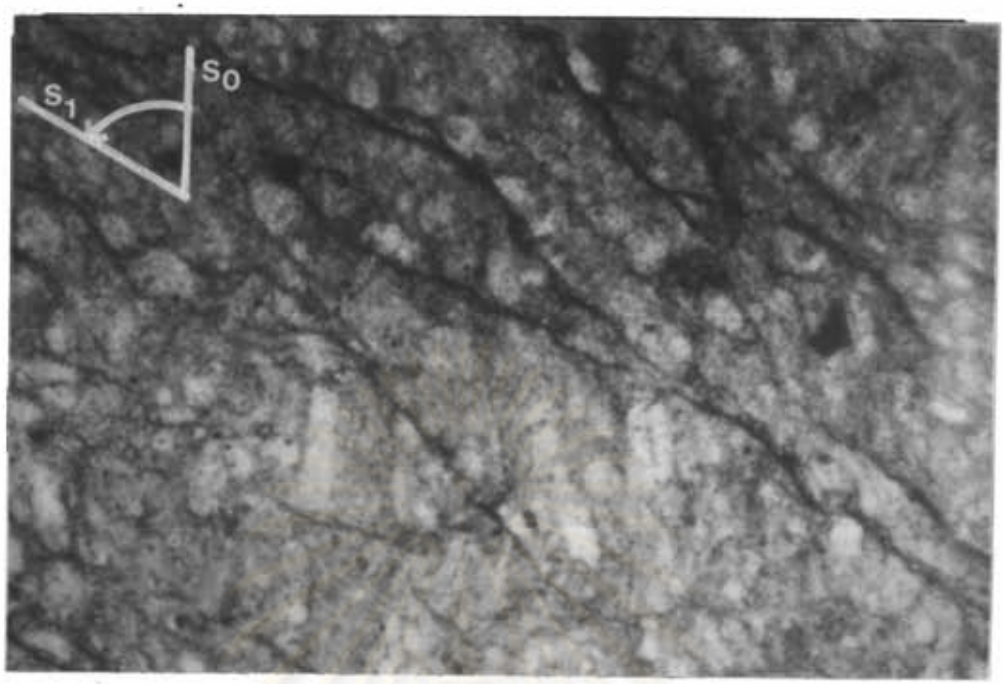

Figure 70 Photomicrograph showing the relationship between the volcaniclastic tuff layers(So)and cleavage surfaces(Sl)at grid reference 24031715, Khao Mai Nuan.(45X,uncrossed nicols)

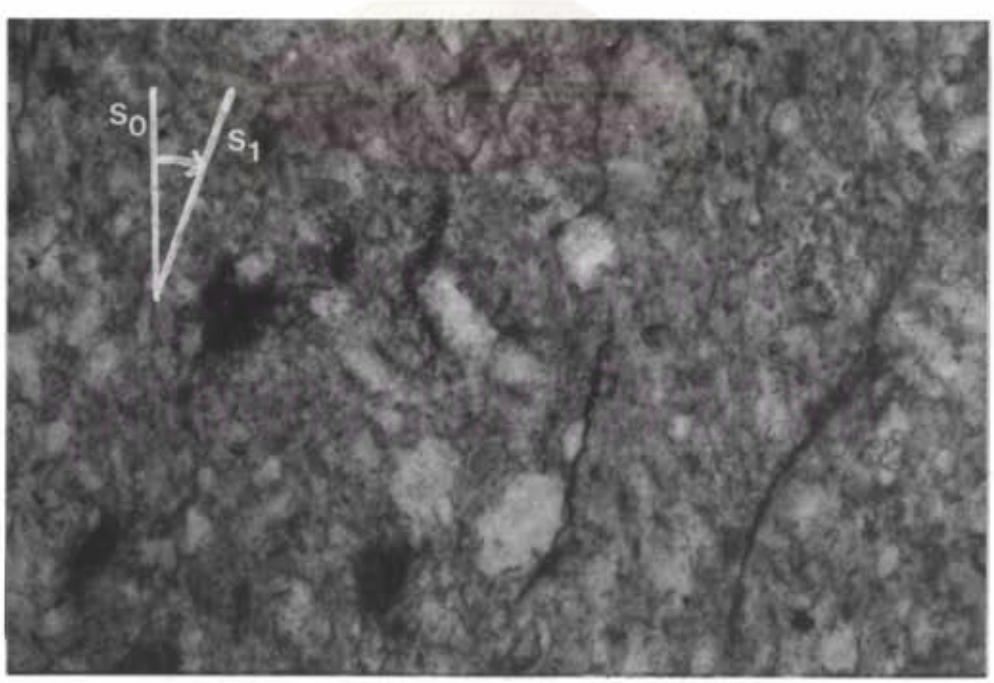

Figure 71 Photomicrograph showing the relationship between the volcaniclastic tuff layers(So)and cleavage surfaces(Sl)at grid reference 30851354, Khao Lom Phat.(45X,uncrossed nicols)

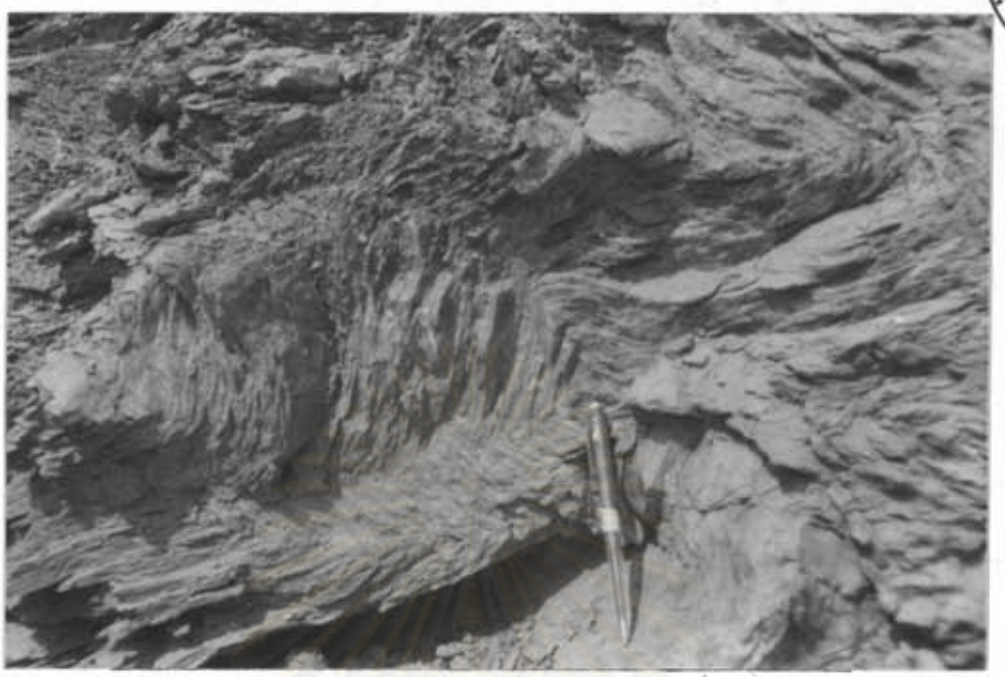

Figure 72 Natural development of conjugate kink fold at grid reference 26331819, Siam City Cement Co. Ltd..

Figure 73 A large kink band developed during the folding of massive bedded limestones at grid reference 32291991, Khao Chan.

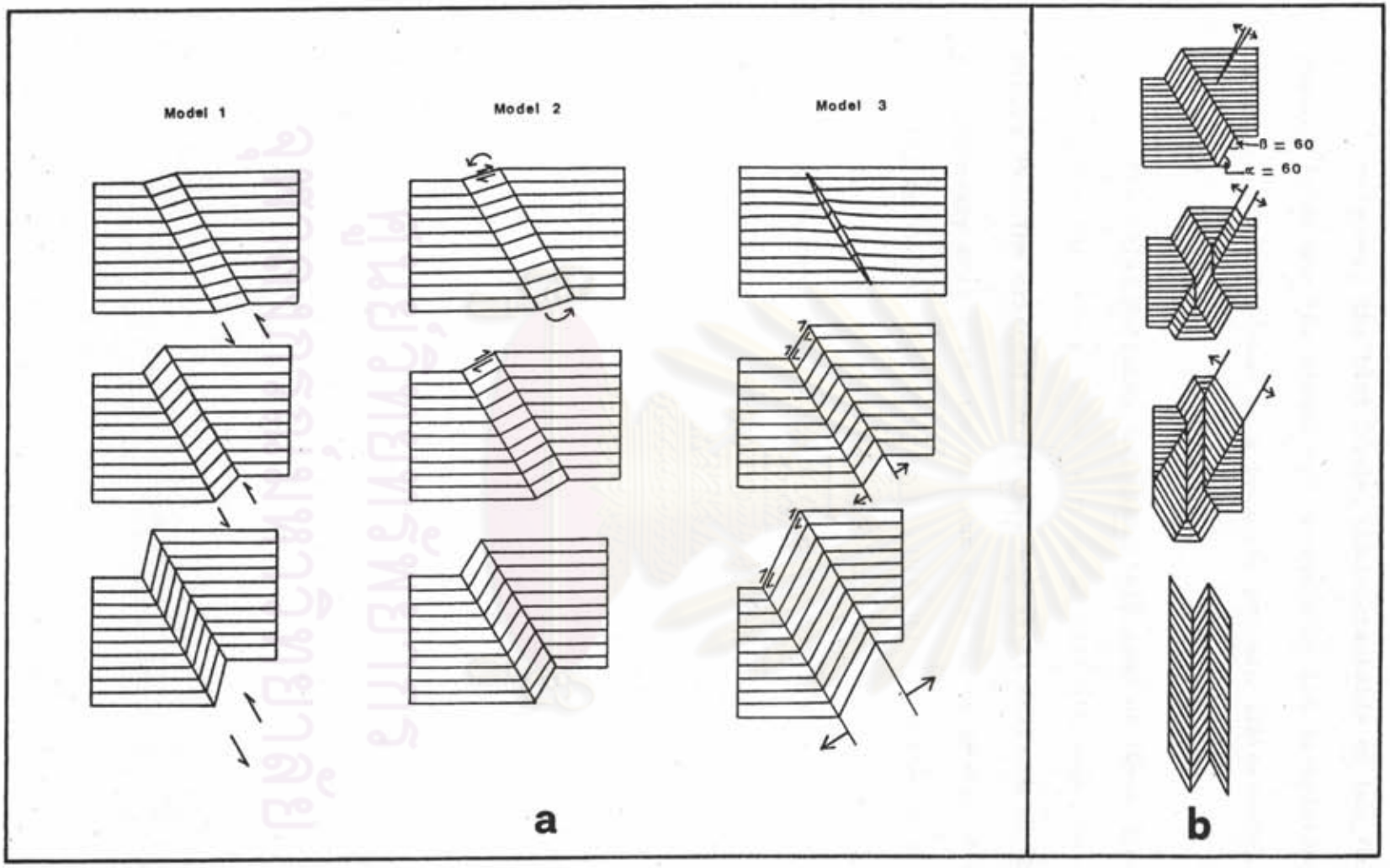

Figure 74 Geometric models for the progressive development of a kink band (a), and the development of chevron folds by the progressive development of one kink band across another (b) (After Ramsay, 1967).

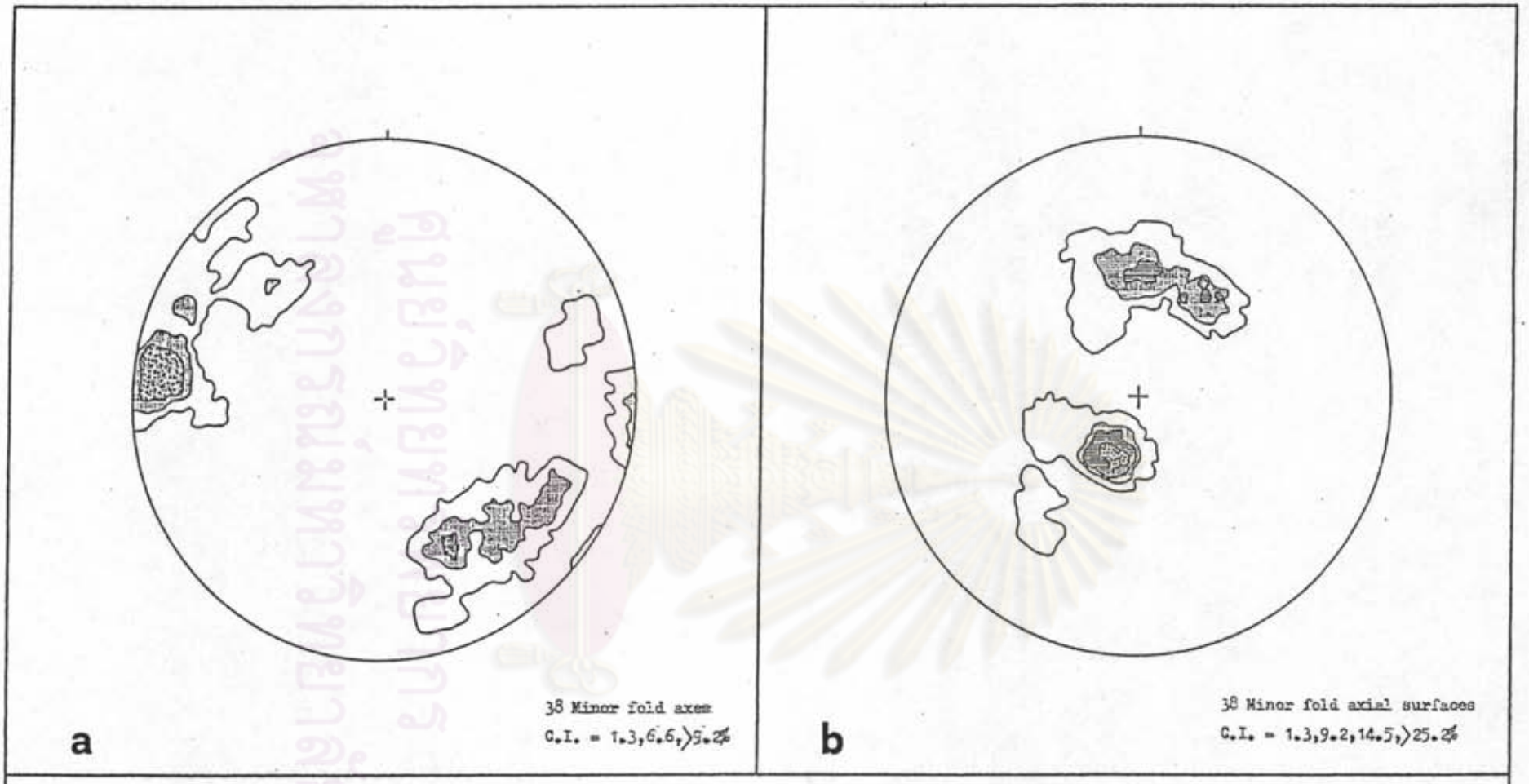

Figure 75 Stereonet plots of (a) minor fold axes, and (b) minor fold axial surfaces in the compounds Siam City Cement Factory.